

Flight Path Curvature Distortion in Side-Looking Airborne Radar Imagery

A quasi-circular piecewise function was fitted to map points transferred from the SLAR imagery in order to correct for flight path curvature distortion.

SLAR (SIDE-LOOKING AIRBORNE RADAR) imagery of surface features of the Earth obtained from aircraft may contain distortions due to (1) yaw, roll, or pitch; (2) change of height; (3) curvature of flight path; and (4) velocity change of the airplane. Previous attempts at correcting these distortions have been made by other authors (Derenyi, 1974; Leberl, 1972). Derenyi and Leberl used two-dimensional polynomials to express overall distortions, with polynomial coefficients

effects of pitch angle and change of height of the airplane) are compensated for electronically, while those due to yaw are compensated for manually. However, effects of flight path curvature and change of velocity still need to be corrected. When the distortions due to curvature are corrected, those from change in velocity are to some extent automatically compensated for, with the remaining distortion becoming primarily local and usually not significant. This is because a

ABSTRACT: Although several of the errors in obtaining SLAR (Side-Looking Airborne Radar) imagery can be substantially corrected electronically, the error due to the curvature of the flight path cannot be. For a 130 km flight over the Alaskan coast this error is estimated to be as much as 2.8 km. A correction method is proposed that requires only a few points identifiable both on the image and on the map. It employs a quasi-circular piecewise function passing through these identifiable points, which enables the image coordinates of any other points to be rapidly converted to map coordinates. Synthetic test data and the Alaskan imagery indicate that the error remaining after applying this curvature correction is about 0.2 km.

found by the comparison of the imagery with a ground map. In this paper we want to present a different approach. The relative merits of our method and their methods will be discussed briefly at the end of this paper.

In a SLAR system such as the Motorola* APS-94 D some distortions (such as the ef-

correction for curvature requires a comparison of the imagery with a ground map for a number of fixed points along the direction of the flight path. Thus, curvature is the one source of distortion that warrants the most attention. In this paper we discuss some aspects of this problem and provide a simple method of approximation as a solution.

The return signal to an aircraft SLAR system comes from strips along the surface of the Earth nearly perpendicular to the flight path.

* The use of the brand name in this report is for identification purposes only and does not imply endorsement by the U.S. Geological Survey.

(This is an adequate approximation for our purposes in the case of real aperture, which we used.) The strips of information are received continuously and are combined into the final image. Regardless of its curvature, the flight path appears as a straight line on the image. Although all remote-sensing flights are intended to follow a great circle, most are influenced considerably by wind and inertial navigation error. Thus, a straight line connecting identifiable points on an image is usually a curve on a map of the ground.

When the airplane is making a left turn, the actual distances parallel to the flight path would be smaller on the left side of the flight path than as seen from the image, and greater to the right of the path. Therefore, we have to bend the image according to the flight path before we can use it. One may ask what quantities remain unchanged during the turning of the airplane. There are only three invariant quantities: the distance, l , from a point to the flight path; the right angle, γ , between the flight path and any scanning line; and the total distance traveled by the airplane.

Any point on the image can be located on the map as follows: first, measure on the image the lateral distance of the point from the flight path and the total distance the aircraft has traveled along the flight path up to that point. Then transfer the point by measuring first the total distance along the actual curved path that was flown and then the lateral distance on a normal to the curve. The essential part of this procedure is to reconstruct the actual flight path on the map. In the following, we will use primed symbols to indicate apparent locations and distances as observed on the image (Figure 1a) and unprimed symbols to indicate the correct values as observed on the map (Figure 1b).

If there exist a number of identifiable fixed points on both the imagery and the map, and if we can construct a function $y = g(x)$ connecting the map points, then we can graphically construct the flight path on the map as follows: let $A' \dots E'$ be identifiable fixed points on the image and $l_1 \dots l_5$ the distance of these points from the flight path $X'X'$ (see Figure 1a). If we draw circles with radii $l_1 \dots l_5$ and centers at $A \dots E$ (that is, the correct map positions), then the envelope of these correct circles gives the actual flight path on the map (XX , see Figure 1b).

To find the map position P , of a general point, which could, for example, be a target on a moving ice floe, draw a line on the

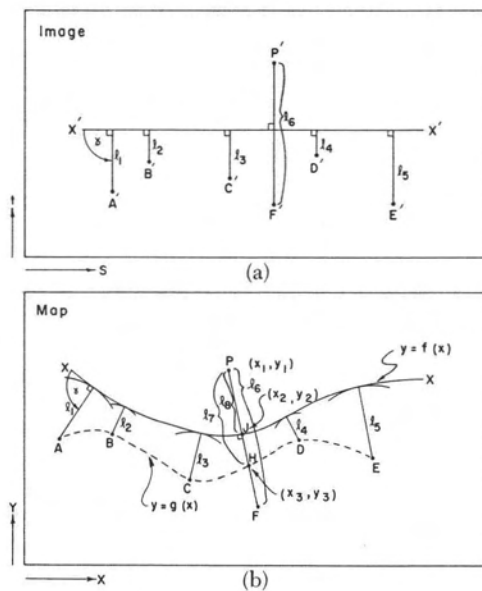


FIG. 1. (a) Geometric relationships between identifiable points and the flight path on the image. (b) Geometric relationships between identifiable points and the flight path on the map.

image through P' perpendicular to $X'X'$ (the apparent flight path) and try to locate an identifiable fixed point, F' , on the line. Next, draw on the map the line PF through F perpendicular to XX , with the length of $PF = l_6$. Then, P is the position of the point on the map. When a large number of points need to be transferred to the map, this graphical method involves considerable manual work. Therefore, it is desirable to make the transfer numerically.

Consider a curve $y = g(x)$ which passes through $ABCDE$ in Figure 1b. If we know l_7 and the location of H (that is, the intersection of PF and $g(x)$) on the map at (x_3, y_3) , the position of P at (x_1, y_1) can be expressed as follows:

$$\begin{aligned} x_1 &= x_3 - f_2' l_7 / \sqrt{1 + (f_2')^2} \\ y_1 &= y_3 + l_7 / \sqrt{1 + (f_2')^2} \end{aligned} \quad (1)$$

where $y = f(x)$ represents XX and $f_2' = dy/dx$ at (x_2, y_2) .

The principal difficulty is in constructing the line PF on the map so that it is normal to the flight path XX , which is as yet unknown. A second difficulty occurs when there is no identifiable point on the line through P normal to the flight path $X'X'$ on the image.

Let us choose $A' \dots E'$ on the image along a straight line parallel to the flight path. We

then assume that $g(x)$ on the map can be approximated by a mathematical function. The given quantities are $(x_3, y_3, g'_3)_A, \dots, (x_3, y_3, g'_3)_E$ corresponding to A, B, C, D, E, etc. It is difficult to find a function that fits all the given quantities, but the curve $g(x)$ can conveniently be fitted piecewise. Fitting with segments of circles appears the simplest and the best way because then all that is needed to find the length of a part of an arc is to use the angle, θ , in Figure 2.

Now the problem has been reduced to the one shown in Figure 2. Given t and s (which is the ratio $(S-S_A)/(S_B-S_A)$ on the image, find $P(X,Y)$ on the map. Since (X_A, Y_A) , (X_B, Y_B) , and (X_C, Y_C) are known, α_A and α_B can be found by fitting with a quadratic through points A, B, and C. A circle can be constructed with center at (X_o, Y_o) that passes through (X_A, Y_A) with slope $m_A = \tan \alpha_A$, and whose radius, through (X_B, Y_B) , is normal to $m_B = \tan \alpha_B$.

$$X_o = \frac{m_B(m_A Y_A + X_A) - m_A(m_B Y_B + X_B)}{m_B - m_A} \tag{2}$$

$$Y_o = \frac{(m_B Y_B + X_B) - (m_A Y_A + X_A)}{m_B - m_A}$$

The circle may or may not go through (X_B, Y_B) since r_A and r_B could be different. One can

introduce the following parametric modification of the circle to avoid this difficulty:

$$X_s = X_o + ur_s \sin \alpha_s \tag{3}$$

$$Y_s = Y_o - ur_s \cos \alpha_s$$

where

$$r_s = (1 - s)r_A + sr_B,$$

$$\alpha_s = (1 - s)\alpha_A + s\alpha_B,$$

$$r_A = \sqrt{(X_A - X_o)^2 + (Y_A - Y_o)^2}, \quad \text{and}$$

$$r_B = \sqrt{(X_B - X_o)^2 + (Y_B - Y_o)^2}.$$

Here we used a simple assumption that the radius of curvature for the arc changes linearly with the angles from r_A to r_B .

To resolve a quadrant ambiguity,

$$u = \begin{cases} +1 & \text{when } \alpha_B > \alpha_A \\ -1 & \text{when } \alpha_B < \alpha_A \end{cases}$$

The case of $\alpha_A = \alpha_B$ will be discussed later.

To accommodate the point P, which is a distance t from the straight line on the image, Equations 3 are slightly altered to give

$$X_p = X_o + (ur_s - kt) \sin \alpha_s \tag{4}$$

$$Y_p = Y_o - (ur_s - kt) \cos \alpha_s$$

where k is the cross-track scale factor between the map and the image, which can be obtained by comparing one or more identifiable length segments on the map with those on the image in the cross-track direction, and t is positive to the left of AB.

When $\alpha_A = \alpha_B$, the curve degenerates to a straight line on the map

$$X_s = X_A + s(X_B - X_A) \tag{5}$$

$$Y_s = Y_A + s(Y_B - Y_A)$$

and the coordinates of P are given by

$$X_p = X_s - v(Y_B - Y_A)$$

$$Y_p = Y_s + v(X_B - X_A)$$

where

$$v = kt/\sqrt{(X_B - X_A)^2 + (Y_B - Y_A)^2} \tag{6}$$

The degeneration of the curve to the straight line cannot be successfully replicated on a computer with a finite word-length because as m_A approaches m_B the distance to (X_o, Y_o) becomes large, as do the radii r_A and r_B , so that one or both of the relations in Equation 4 become numerically

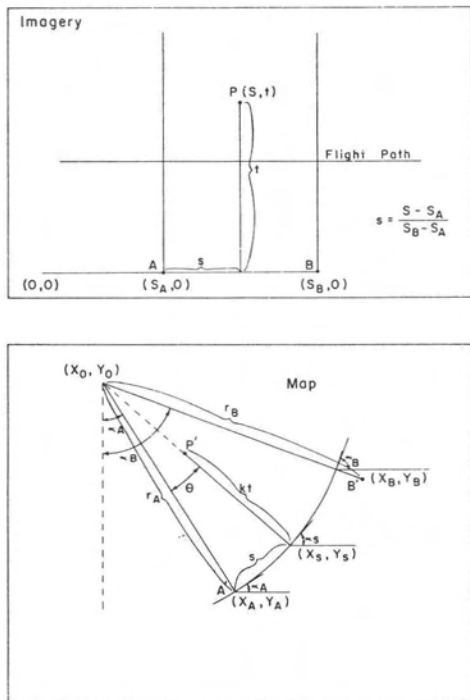


FIG. 2. Piecewise fitting with circular curves between two identifiable points on the map.

ill-conditioned. It is therefore appropriate to switch to Equations 5 and 6 before the two slopes become identical.

It may be shown, where D is the distance between the point given by Equations 4 and the point given by Equations 6, that the relative error obeys the relation

$$\frac{D}{d} < |\Delta m| \left(\frac{1}{8} + \frac{|kt|}{2d} \right)$$

where d is the distance from A to B , and

$$\Delta m = \frac{(m_B - m_A) d^2}{(\Delta X + m_B \Delta Y) (\Delta X + m_A \Delta Y)}$$

in which $\Delta X = X_B - X_A$ and $\Delta Y = Y_B - Y_A$.

For $|kt| \leq 10d$, the relative error does not exceed $41/8 |\Delta m|$. Then, for example, $|\Delta m| < 0.0002$ produces a relative error less than 0.001 when Equations 6 are used instead of Equations 4. This avoids the ill-conditioning in Equations 4 even on a computer with a mantissa length as short as 20 bits.

The above method can be used when r_A and r_B are equal or only slightly different (otherwise the radius and its tangent will not be quite perpendicular and error is introduced). However, some uncertainty arises in trying to find the slope of a curve that is fitted to a number of discrete points either graphically or numerically. Another requirement is that a line normal to $g(x)$ is also nearly normal to the flight path.

The above method was tested two ways: (1) a fictitious image and a corresponding fictitious map were made up in which the flight path is a simple mathematical function. Thus, an exact solution exists for Equation 1. The results from the method using Equation 4 were compared with the exact solution; and (2) real SLAR data with corresponding ground maps were used for comparison with the method. The details of the two methods are as follows:

(1) For a mathematical function as a flight path on the map, $y = 0.1x^2$ was used with $0 \leq x \leq 1$. This function makes a total turning of about 11° , which is roughly twice the amount of actual turning of the airplane based on the SLAR data we have. Three identifiable points at $x = 0, 0.5, \text{ and } 1$ were used to produce two separate, nearly circular curves by the use of Equations 2. For a point (x, y) on $y = 0.1x^2$, it is simple to find the length of the curve s from $(0, 0)$ to (x, y) . Construct a normal at (x, y) and measure t away from it to end up at (X_p, Y_p) . The point (X_p, Y_p) corresponds exactly to (S, t) on the image. The point (x, t) is specified arbitrarily to get (S, t) and (s, t) . The map coordinates of a

point that measures (S, t) on the image are calculated using Equations 4. This is done for $x = 0.1, 0.2, \dots, 0.9, 1.0$ and $t = 0, 0.2, 0.4, \dots, 1.0$. The numbers are then compared with the exact solution that follows:

$$X_p = x - t/\sqrt{1 + (1/0.04)x^2}$$

$$Y_p = 0.1x^2 + t/\sqrt{1 + 0.04x^2}$$

In all cases they differ by about 10^{-4} or less. This is very good agreement because for an image 1 m long and 40 cm wide the difference corresponds to an error of 1/20 of a millimetre (since the error is only 5×10^{-5} for $0 \leq x \leq 1$ and $t \leq 0.4$), which is well within the error of measuring distances on an image.

(2) A SLAR image of the Alaska coast-ice shear zone made by W. F. Weeks and W. J. Campbell (USGS-CRREL report in preparation) is used here with a topographic map (U.S. Geological Survey, Alaska Topographic Series, Barrow, Meade River, and Wainwright Sections, 1:250,000) made in 1955. Ten strips of images are available. The one strip showing the greatest amount of land was chosen for the test. We picked five identifiable points along the flight path and made four nearly circular curves for the map. The five points cover about 130 km in real distance and 52 cm on the map. Five more identifiable points were picked for testing, all far from the flight path. (See Figure 3.)

The coordinates of five control points as well as five testing points are shown in Table 1.

Column (2) in Table 1 is used for the calculation of Equation 2. The m 's in Equation 2 are found by fitting a quadratic through three points, with the point in question in the middle, if it is not an end point. (An end point shares the same quadratic with the point next to it.) Thus, four sets of values for (X_p, Y_p) can be obtained from the five points in column (2). Column (1) provides four sets of values for $S_B - S_A$; namely, 13.4,

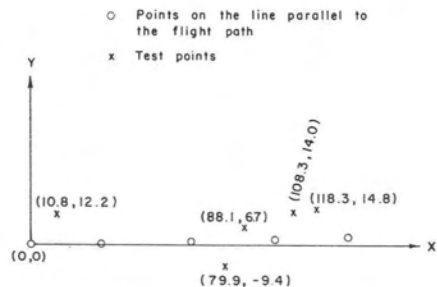


FIG. 3. Orientation of the coordinate system for the SLAR data (units in km).

TABLE 1. COORDINATES OF FIVE CONTROL POINTS AND FIVE TESTING POINTS

Five Control Points			Five Testing Points		
(1) Image, (x,y) or (S,t)	(2) Map (X,Y)	(3) Image, (x,y) or (S,t)	(4) Image (s,t)	(5) Map, Measured	(6) Map, Calculated
(0,0)	(0,0.1)	(4.6, 7.8)	(.3433, 7.80)	(6.8, 7.7)	(6.42, 7.81)
(13.4,0)	(18.5,0)	(40.7, 3.45)	(.6352, 3.45)	(55.5, 4.25)	(55.26, 4.20)
(30.6,0)	(41.7,0.4)	(37.2,-6.5)	(.415,-6.5)	(50.3,-5.9)	(50.80,-5.88)
(46.5,0)	(63.2,1.0)	(50.55, 7.7)	(.291, 7.7)	(68.2, 8.8)	(68.57, 8.89)
(60.4,0)	(82.6,1.75)	(55.1, 7.9)	(.6187, 7.9)	(74.5, 9.3)	(74.89, 9.33)

Note: Units of the above coordinates are in terms of 1/4 of an inch. To change the map scale to kilometers, the scale factor is 20 km/12.6 units.

17.2, 15.9, and 13.9. Column (3) provides the values of S and Column (4) gives the values of (s,t) where $s = (S - S_A)/(S_B - S_A)$. Equation 4 is used for the calculation of the coordinates of the five test points, using $k = 1$. The calculated results are shown in column (6). Figure 3 shows the orientation of the coordinate system.

Column (5) and Column (6) in Table 1 show that the calculations agree very well with measurements in the direction normal to the flight path, the maximum difference being 0.2 km (after applying the scale factor of 20 km/12.6 units). However, the maximum difference in the direction parallel to the flight path is about 0.7 km. It was discovered that this discrepancy comes from the fact that the distortion due to the yaw of the airplane was not adequately compensated for by the SLAR equipment. However, the image used is as good as the present state of the art permits.

It seems likely that in the future the effects of yaw and of change in velocity can be accurately compensated for electronically because the correction involves mechanical elements that can be controlled electronically (the angle of the trace and the speed of the

film-drive motor). These compensations can be performed while the film is being taken. The curvature effect, on the other hand, cannot be compensated for until the whole film has been made, and it is doubtful that compensation can be accomplished electronically unless at least two more degrees of freedom can be introduced to the film take-up spool, which illustrates the necessity for an adequate method to deal with the curvature effect.

What are the consequences of not using this "curvature correction" at all? Tests show that failure to make the correction does not affect distances parallel to the flight path significantly, but that it affects distances normal to the flight path a great deal. Instead of an error of 0.2 km on the map, an error of 2.8 km occurs for the imagery from the APS-94 D. Therefore, the "curvature correction" is significant in the use of SLAR imagery.

A comparison has been made between our method, Derenyi's method, and Leberl's method using the same control points and testing points as shown in Table 1. The results are tabulated in Table 2.

Column (2) of Table 2 is obtained by the use of the following linear transformation:

TABLE 2. A COMPARISON OF RESULTS FROM DIFFERENT METHODS

Map Coordinates, Measured	Calculated Coordinates			
	(1) Ling, et al.	(2) Derenyi	(3) Leberl	(4) Linear Trans. Only
(6.8, 7.70)	(6.42, 7.81)	(9.21, 21.63)	(9.21, 28.80)	(6.08, 10.89)
(55.5, 4.25)	(55.26, 4.20)	(70.97, 10.96)	(70.97, 12.48)	(55.56, 5.93)
(50.3,-5.90)	(50.80,-5.88)	(36.10,-16.96)	(36.10,-12.02)	(51.05,- 7.77)
(68.2, 8.80)	(68.57, 8.89)	(105.41, 23.27)	(105.41, 30.95)	(68.92, 12.01)
(74.5, 9.30)	(74.89, 9.33)	(116.14, 24.04)	(116.14, 32.19)	(75.14, 12.41)

Note: Units of the above coordinates are in terms of 1/4 of an inch. To change the map scale to kilometers, the scale factor is 20 km/12.6 units.

$$X = Ax - By + C_1 \quad (7a)$$

$$Y = Bx + Ay + C_2 \quad (7b)$$

and a five term polynomial correction:

$$dX = A_1 + A_2X + B_1Y + B_2XY + A_3X^2 \quad (8a)$$

$$dY = C_3 + D_1Y + C_4X + D_2XY + C_5X^2 \quad (8b)$$

Column (3) is obtained by using Equations 7a, 7b, and a slightly different polynomial for dY :

$$dY = C_3 + D_1Y + C_4X + D_2Y^2 + C_5X^2 \quad (9)$$

Column (4) is obtained by using Equations 7a and 7b only.

Table 2 shows that the results from Derenyi's method, as well as Leberl's method, do not compare favorably with the measured map coordinates. Even the results from linear transformation only ($dX = dY = 0$) are better than those with the use of Equations 8a, 8b, and 9. The reason is that Equations 8a, 8b, and 9 are two-dimensional curves, the fitting of which requires enough data points throughout a two-dimensional domain in order to give good results. But the five control points used are almost on a straight line (see Figure 3), and therefore the two-dimensional polynomial fittings fail

to produce good agreement for the five testing points, which are quite far from the control points.

Our method is an approximation to the mathematical solution of Equation 1 for the problem of curvature distortion which relates the distortion of the image to the turning of an airplane. It is not just a curve fitting. Thus, it can give very reasonable results without the need of a two-dimensional set of control points. It does, however, need several identifiable points on a line parallel to the flight path.

ACKNOWLEDGMENTS

The authors are very grateful to Dr. Wilford F. Weeks of the U.S. Army Cold Regions Research and Engineering Laboratory for his helpful comments.

REFERENCES

- Derenyi, E. E. 1974. SLAR Geometric Test. *Photogrammetric Eng.*, Vol. 40, No. 5.
 Leberl, F. 1972. Evaluation of Single Strips of Side-Looking Radar Imagery, Invited Paper for Commission IV, Twelfth Congress of the International Society of Photogrammetry, Ottawa.

(Received March 23, 1977; revised and accepted July 10, 1978)

Forthcoming Articles

- Louis F. Dellwig and Janét E. Bare*, A Radar Investigation of North Louisiana Salt Domes.
Frederick J. Doyle, A Large Format Camera for Shuttle.
Patricia T. Gammon and Virginia Carter, Vegetation Mapping with Seasonal Color Infrared Photographs.
Shin-yi Hsu, Texture-Tone Analysis for Automated Land-Use Mapping.
Takenori Takamoto, Ph.D., Bernard Schwartz, M.D., Ph.D., and G. T. Marzen, Ph. D., Stereo Measurement of the Optic Disc.
R. L. Talerico, J. E. Walker, and T. A. Skratt, Quantifying Gypsy Moth Defoliation.
Compton J. Tucker, A Comparison of Satellite Sensor Bands for Vegetation Monitoring.
Mike E. White, Reservoir Surface Area for Landsat Imagery.
C. H. Whitlock, W. G. White, J. W. Usry, and E. A. Gurganus, Penetration Depth at Green Wavelengths in Turbit Waters.